

DD

LBL-36274
UC-406



Lawrence Berkeley Laboratory

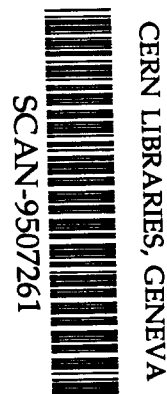
UNIVERSITY OF CALIFORNIA

Presented at the IEEE 1994 Nuclear Science Symposium, Norfolk, VA, Nov. 1-5, 1994, and to be published in the Proceedings

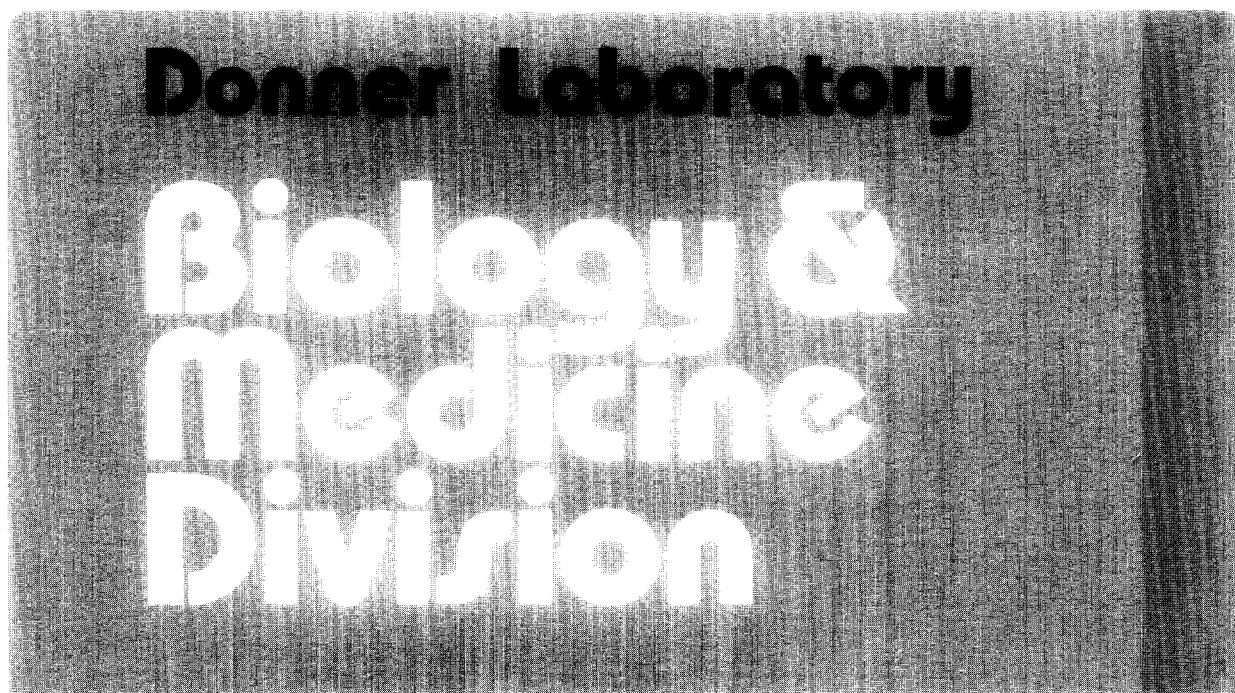
A Room Temperature LSO/PIN Photodiode PET Detector Module that Measures Depth of Interaction

W.W. Moses, S.E. Derenzo, C.L. Melcher, and R.A. Manente

November 1994



SW 95 34



DISCLAIMER

This document was prepared as an account of work sponsored by the United States Government. Neither the United States Government nor any agency thereof, nor The Regents of the University of California, nor any of their employees, makes any warranty, express or implied, or assumes any legal liability or responsibility for the accuracy, completeness, or usefulness of any information, apparatus, product, or process disclosed, or represents that its use would not infringe privately owned rights. Reference herein to any specific commercial product, process, or service by its trade name, trademark, manufacturer, or otherwise, does not necessarily constitute or imply its endorsement, recommendation, or favoring by the United States Government or any agency thereof, or The Regents of the University of California. The views and opinions of authors expressed herein do not necessarily state or reflect those of the United States Government or any agency thereof or The Regents of the University of California and shall not be used for advertising or product endorsement purposes.

Lawrence Berkeley Laboratory is an equal opportunity employer.

This publication has been reproduced from the best available copy

**A Room Temperature LSO/PIN Photodiode PET
Detector Module that Measures Depth of Interaction**

W.W. Moses and S.E. Derenzo

Life Sciences Division
Lawrence Berkeley Laboratory
University of California
Berkeley, California 94720

C.L. Melcher and R.A. Manente

Schlumberger-Doll Research
Ridgefield, Connecticut 06877

November 1994

This work was supported by the Director, Office of Energy Research, Office of Health and Environmental Research, Medical Applications and Biophysical Research Division, of the U.S. Department of Energy under Contract No. DE-AC03-76SF00098, and by the National Institutes of Health, National Heart, Lung, and Blood Institute, National Cancer Institute, and National Institute of Neurological Disorders and Stroke under Grants No. P01-HL25840, No. R01-CA48002, and No. R01-NS29655.



recycled paper

A ROOM TEMPERATURE LSO / PIN PHOTODIODE PET DETECTOR MODULE THAT MEASURES DEPTH OF INTERACTION*

W. W. Moses[§], S. E. Derenzo[§], C. L. Melcher[†], and R. A. Manente[†],

[§]Lawrence Berkeley Laboratory, University of California, Berkeley, CA 94720

[†]Schlumberger-Doll Research, Ridgefield, CT 06877

Abstract

We present measurements of a 4 element PET detector module that uses a 2x2 array of 3 mm square PIN photodiodes to both measure the depth of interaction (DOI) and identify the crystal of interaction. Each photodiode is coupled to one end of a 3x3x25 mm LSO crystal, with the opposite ends of all 4 crystals attached to a single PMT that provides a timing signal and initial energy discrimination. Each LSO crystal is coated with a “lossy” reflector, so the ratio of light detected in the photodiode and PMT depends on the position of interaction in the crystal, and is used to determine this position on an event by event basis. This module is operated at +25° C with a photodiode amplifier peaking time of 2 μs. When excited by a collimated beam of 511 keV photons at the photodiode end of the module (*i.e.* closest to the patient), the DOI resolution is 4 mm fwhm and the crystal of interaction is identified correctly 95% of the time. When excited at the opposite end of the module, the DOI resolution is 13 mm fwhm and the crystal of interaction is identified correctly 73% of the time. The channel to channel variations in performance are minimal.

1. INTRODUCTION

It is becoming increasingly important to develop a PET detector module that is capable of measuring the distance that the 511 keV annihilation photons penetrates into the detector ring before interacting (*i.e.* the depth of interaction) on an event by event basis. This penetration leads to a resolution degradation artifact (known as radial elongation) whose severity increases as the angle of incidence of the annihilation photon increases (where the angle of incidence is defined as the angle between the direction of travel of the photon and the normal to the front surface of the detector module). While this artifact is barely noticeable in whole body PET cameras (ring diameter ≥80 cm), it causes significant degradation towards the edge of the field of view in cerebral cameras (ring diameter 50–80 cm), dominates the resolution in small animal PET cameras (ring diameter <50 cm), and could be a “show-stopper” for disease specific PET camera geometries where the object to be imaged fills the detector aperture, such as in Positron Emission Mammography cameras [1, 2].

We have previously characterized [3] a PET detector module that measures depth of interaction on an event by event basis using the method shown in Figure 1. The module consists of

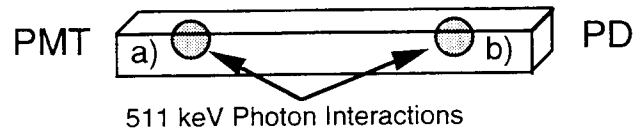


Figure 1: Depth of interaction measurement method. The scintillator crystal is coupled to a photomultiplier (PMT) and a photodiode (PD) and the other faces coated with a “lossy” reflector. Interactions near the PMT, as in a), result in a large PMT signal and a small PD signal. Interactions near the PD, as in b), result in a small PMT signal and a large PD signal.

a 3x3x30 mm BGO scintillator crystal that is coupled on one 3x3 mm face to a silicon photodiode and on the opposing face to a photomultiplier tube. The other faces are coated with a “lossy” reflector so that the signals observed in the photodiode and the photomultiplier tube depend on the depth of the 511 keV photon interaction in the scintillator crystal, and the ratio of these two signals is used to determine this depth.

This module had sufficiently good depth of interaction measurement resolution (5–8 mm fwhm) to effectively eliminate radial elongation in a cerebral PET camera and sufficiently high signal to noise ratio to correctly identify the crystal of interaction. The detector modules fit together without gaps to form a multi-ring tomograph and the cost of the necessary components is reasonable. However, the modules must be operated at –20° C to have sufficiently high signal to noise ratio to achieve the above performance characteristics (the light output of BGO increases by a factor of 1.7 compared to room temperature [4]). Cooling the gantry adds a relatively small cost to a PET camera, but makes servicing the camera extremely difficult and thus limits the commercial utility of the design. In addition, this test module had only one crystal, causing concern about crystal to crystal variations and the ability of the module to simultaneously identify the crystal of interaction and measure the depth of interaction.

In this paper we propose a similar module that operates at room temperature. The requisite signal to noise ratio is obtained by using LSO scintillator [5], whose light output is approximately 4 times that of BGO but whose emission spectrum is not as good a match to the photodiode spectral response. A four element detector module is constructed and characterized for both its depth of interaction measurement resolution and crystal misidentification fraction.

2. EXPERIMENTAL APPARATUS

To test this detector concept, we constructed a module consisting of a two by two array of 3x3x25 mm LSO crystals, coupled on one end to a 3/8 inch square photomultiplier tube

* This work was supported in part by the U.S. Department of Energy under Contract No. DE-AC03-76SF00098, and in part by Public Health Service Grant Nos. P01 25840, R01 CA48002, and R01 NS29655.

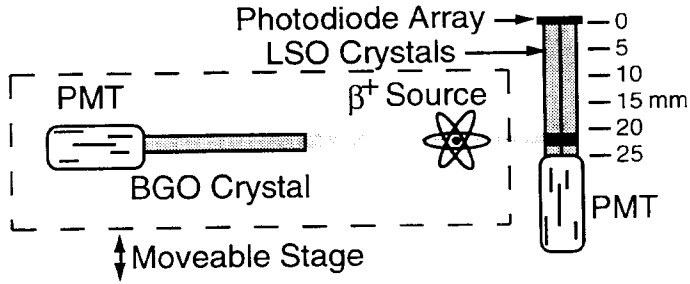


Figure 2: Experimental set-up. The β^+ source, 3x3x30 mm BGO crystal, and PMT provide an electronically collimated beam (2.5 mm fwhm) whose position is adjusted by moving the stage (left/right and in/out of the page).

and on the opposite end to a 2 by 2 array of 3x3 mm silicon photodiodes. The PIN photodiodes are Hamamatsu S-2506 (2.77 mm square active area, 100 μm depletion thickness) devices mounted in a special package to allow close coupling to the scintillator crystal. The “lossy” reflector is made by sanding the LSO crystal before applying a white reflective coating. For all subsequent, the photodiode is biased with +80 V and the assembly operated at room temperature (+25° C). Under these operating conditions, the capacitance is 9 pF and the dark current is <100 pA.

A custom integrated circuit amplifier array [6] with a 2 μs peaking time processes the photodiode signal, and the noise (520 electrons (e^-) fwhm) is measured using a calibrated test pulse. This is significantly larger than the 330 e^- fwhm noise achieved earlier [3] due to the higher operating temperature and shorter shaping time used in the present work.

This test module is illuminated with an electronically collimated beam of annihilation photons from a ^{68}Ge source, as shown in Figure 2. The position of the beam (in 2 dimensions) is varied by moving the entire collimation apparatus, allowing a 2.5 mm fwhm portion of the test module to be excited at an arbitrary depth of interaction. The depth coordinate system is chosen such that 0 mm corresponds to the end of the LSO crystal closest to the photodiode and 25 mm is the end closest to the photomultiplier tube.

3. EXPERIMENTAL MEASUREMENTS

The detector module must be calibrated (on a crystal by crystal basis) in order to determine how the ratio between the photodiode and photomultiplier tube signals depends on interaction depth. To do this, the module is excited from the side with the electronically collimated beam as shown in Figure 2. Whenever a coincidence between the photomultiplier tubes is detected, the 4 signals observed in the photodiode array and the signal in the “test module” photomultiplier tube are simultaneously digitized and read into a computer. The pulse height spectrum observed in each channel of the photodiode array and photomultiplier tube is obtained as a function of excitation position, and the centroid of the 511 keV photopeak in each of the 5 detectors is computed at each position.

The centroid of the 511 keV photopeak observed in the photomultiplier tube is a smooth function of position

(reasonably linear but with a small exponential term) that varies over a 5:1 range. A clear photopeak centered at 1200 e^- is also observed in the photodiode array when excited at the photodiode end of the LSO crystal (*i.e.* closest to the patient), but the photopeak cannot be separated from the noise when the module is excited at the opposite end of the LSO crystal.

Because of different quantum efficiencies, detector and amplifier gains, and ADC conversion factors, a given optical signal produces different measured signals in the 5 photodetectors (4 photodiodes and 1 photomultiplier tube), or

$$PD_i = k_i \mathcal{L}$$

$$PMT = k_{PMT} \mathcal{L}, \quad (1)$$

where \mathcal{L} is the amount of light impinging on the photodetector. In order to compare the measured photodiode and photomultiplier tube outputs and compute a position estimator, it is necessary measure the ratios $K_i = k_{PMT} / k_i$. To do this, we invoke a symmetry argument and assume that the light output from either 3x3 mm face of the LSO crystal depends only on the distance of the interaction from the crystal face, or

$$\mathcal{L}(x) = \mathcal{L}(25-x), \quad (2)$$

where $\mathcal{L}(x)$ is the amount of light impinging on the photodiode when excited by 511 keV photons at a depth of x mm. We then obtain the gain normalization factor by dividing

$$K_i = \frac{PMT(22)}{PD_i(3)}, \quad (3)$$

where PMT(22) is the centroid of the 511 keV photopeak in the photomultiplier tube when the detector is excited at a depth of 22 mm and $PD_i(3)$ is the 511 keV photopeak centroid in photodiode i when the detector is excited at a depth of 3 mm. The photodetector signals are then be converted into a equal energy scale and directly compared using these K_i .

The sharing of the signal between the photomultiplier tube and the photodiode has consequences for the trigger. A trigger threshold at a fixed energy deposit is desired, but only the photomultiplier tube output is available to the trigger. Therefore, a preliminary trigger must be made based on the photomultiplier tube, then the photomultiplier tube and photodiode are read out and converted into a equal energy scale (using the method described above) before a total energy deposit threshold is applied to the sum. In these tests, the photomultiplier tube trigger threshold corresponds to 250 keV energy deposit when the test module is excited at 2 mm depth and 50 keV when excited at 23 mm depth, and an energy threshold of 250 keV applied to the summed signals.

To compute the crystal misidentification fraction, the height of the moveable stage in Figure 2 is adjusted (*i.e.* in or out of the page) so that the beam of 511 keV photons detector array is incident on either the lower or upper pair of LSO crystals. If a coincidence between the photomultiplier tubes is detected, the 4 signals observed in the photodiode array and in the “test module” photomultiplier tube are simultaneously digitized, read into a computer, normalized, and the photodiode with the largest signal (after applying the gain correction factors K_i) considered to be the crystal of interaction. This identification is considered “correct” if one of the two crystals in the path of the beam was labeled as the crystal of interaction. When excited at a depth of 3 mm (the patient end), the

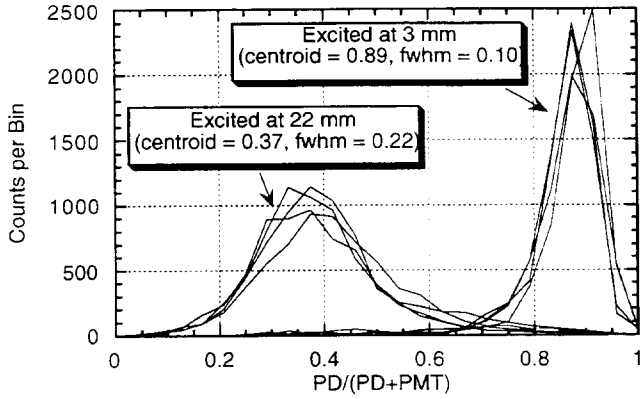


Figure 3: Distribution of the ratio $PD / (PD+PMT)$ with the test module excited at a fixed positions of 3 and 22 mm. The four “traces” in each peak correspond to the four individual crystals.

crystal of interaction is “correctly” identified 95% of the time, and when excited at a depth of 22 mm (the PMT end), the crystal of interaction is “correctly” identified 73% of the time.

The interaction position is measured on an event by event basis by computing a position estimator, defined as the fraction of the summed output from the two photodetectors that is observed by the photodiode, or $\Gamma = PD / (PD+PMT)$. Here PD is the largest pulse height (after normalization) observed in the photodiode array and PMT is the re-scaled pulse height observed by the photomultiplier tube. Figure 3 plots this ratio for all 4 photodiode channels with the test module excited at interaction depths of 3 and 22 mm. This plot shows that the centroid of the estimator depends strongly on position and that the estimator distributions are quite similar for all four photodiode channels (suggesting that the channel to channel variations in the optical properties are small). In addition, the width of the estimator (which is related to the error in the position estimation) is significantly greater when excited at a depth of 22 mm than it is when excited at 3 mm.

The collimated excitation beam is scanned along the test module, and at each depth of interaction the centroid and fwhm of the depth estimator $\Gamma = PD / (PD+PMT)$ are computed.

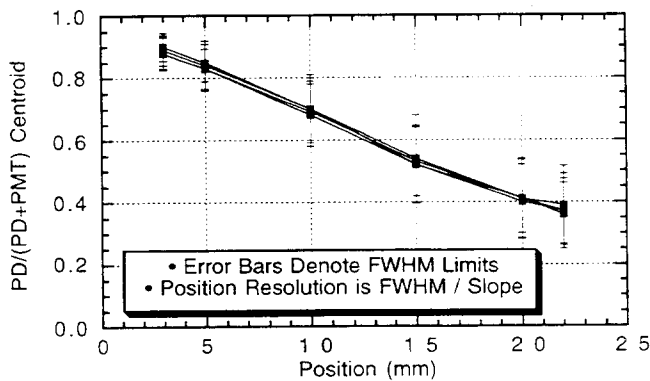


Figure 4: Value of the position estimator $PD / (PD+PMT)$ and the sum signal $PD+PMT$ versus depth of interaction. The four “traces” correspond to the four individual crystals.

Figure 4 plots these measurements for all four detector elements as a function of depth of interaction, with the fwhm of the depth estimator represented as error bars on the estimator. The centroid of the estimator Γ is linearly dependent on depth, and the fwhm of this estimator increases with increasing depth (since the noise in the photodiode is constant but the signal decreases with increasing depth). Dividing the fwhm of the depth estimator by the slope yields the depth of interaction measurement resolution, which varies from 4 mm fwhm at a depth of 3 mm (the end near the photodiode / patient) to 13 mm fwhm at a depth of 22 mm. Again, the dependence of the centroids and widths on position is virtually identical in all four channels. This uniformity is very desirable for a module composed of a large number of crystals (64 has been proposed in [3]), as it implies that the only channel specific correction that needs to be applied is the overall gain factor K_j , as opposed to a channel dependent estimator (Γ) versus position (x) map.

4. PREDICTED MEASUREMENT RESOLUTION

The position resolution R obtained for a signal S (defined as the photopeak position observed in the photodiode when excited at the photodiode end), photodiode noise N , and “light loss” α (defined as the ratio between photopeaks observed when excited at either end of the crystal, with $\alpha \geq 1$) can be estimated as follows. The average photopeak signal observed in each photodiode is assumed to vary linearly with excitation position, ranging from a value of S when excited at the end of the crystal closest to the photodiode to a value of S/α when excited at the end furthest from the photodiode. Thus, position dependent signals observed in the photomultiplier tube and photodiode are

$$PD(x) = \frac{S}{\alpha} [(\alpha - 1)(1 - x) + 1] \quad (4)$$

and

$$PMT(x) = \frac{S}{\alpha} [(\alpha - 1)x + 1], \quad (5)$$

where the position variable x is normalized ($0 \leq x \leq 1$, with $x=0$ at the photodiode end). The centroid of the estimator $\Gamma(x)$ is

$$\Gamma(x) \equiv \frac{PD(x)}{PD(x) + PMT(x)} = \frac{(\alpha - 1)(1 - x) + 1}{\alpha + 1}, \quad (6)$$

so the slope of the estimator is given by

$$\frac{\partial \Gamma(x)}{\partial x} = \frac{1 - \alpha}{1 + \alpha}. \quad (7)$$

If the photomultiplier tube noise is assumed to be much less than the photodiode noise, the width of the estimator $\Delta \Gamma(x)$ is

$$\Delta \Gamma(x) \equiv N \frac{\partial \Gamma}{\partial PD} = \frac{PMT}{[PD + PMT]^2} = \frac{N}{S} \frac{\alpha [(\alpha - 1)x + 1]}{[\alpha + 1]^2} \quad (8)$$

and the position resolution $R(x)$ is given by

$$R(x) = \frac{\Delta \Gamma(x)}{\partial \Gamma / \partial x} = \frac{N}{S} \frac{\alpha [(\alpha - 1)x + 1]}{1 - \alpha^2} \equiv \frac{N}{S} G(x, \alpha). \quad (9)$$

Note that since x has been rescaled to be between 0 and 1, equation 9 gives the position resolution $R(x)$ as a fraction of the crystal length.

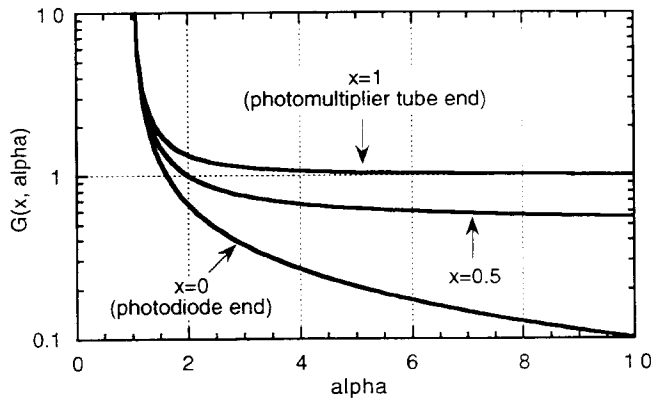


Figure 5: Dependence of the depth of interaction measurement resolution on position x ($0 \leq x \leq 1$) and α (the light loss factor). See equation 9 for definition of $G(x, \alpha)$.

Equation 9 predicts that the position resolution improves linearly as the signal to noise ratio N/S improves. The dependence on α becomes clearer when the function $G(x, \alpha)$ is shown graphically for several values of x , as in Figure 5. When the light loss ratio α is less than two (*i.e.* the light collection is relatively uniform), the position resolution is poor for all excitation positions x . For values of $\alpha \geq 2$, the position resolution improves like $1/\alpha$ when excited at the photodiode end and is approximately constant when excited at the photomultiplier tube end. Therefore, one expects increasing differences in the position resolution at the two ends of the crystal as the light loss ratio α increases.

The theoretical resolutions predicted by equation 9 are similar to those observed experimentally, although the experimental values are slightly higher. The BGO detector described earlier [3] has a signal S of $1250 e^-$, a noise N of $330 e^-$ fwhm, a light loss ratio α of 3, and a crystal length of 30 mm. Based on these values, Equation 9 predicts position resolutions of 3 mm fwhm when excited at $x=0$ and 9 mm fwhm when excited at $x=1$, while the experimentally measured resolution were 5 mm and 8 mm fwhm. Similarly, this LSO detector has $S=1200 e^-$, $N=520 e^-$ fwhm, $\alpha=5$, and a 25 mm length, leading to predicted position resolutions of 2 mm and 11 mm fwhm (when excited at $x=0$ and $x=1$ respectively), as compared to experimentally measured resolutions of 4 mm and 13 mm fwhm. These results are shown in Table 1.

Table 1: Comparison of predicted and measured depth of interaction measurement resolution for the two detector modules.

	BGO, -20°C	LSO, $+25^\circ \text{C}$
α (Light Ratio)	3	5
S (Max. Signal)	$1250 e^-$	$1200 e^-$
N (PD Noise)	$330 e^-$ fwhm	$520 e^-$ fwhm
Length of Crystal	30 mm	25 mm
Predicted (PD end)	3 mm fwhm	2 mm fwhm
Measured (PD end)	5 mm fwhm	4 mm fwhm
Predicted (PMT end)	9 mm fwhm	11 mm fwhm
Measured (PMT end)	8 mm fwhm	13 mm fwhm

The influence of the depth of interaction measurement resolution on the reconstructed point spread function (PSF) has been previously reported for a PET camera with 60 cm ring diameter and 3 mm wide BGO crystals [7]. Briefly summarized, Monte Carlo simulation predicts that a depth measurement resolution of 10 mm fwhm reduces the blurring due to radial elongation by a factor of two, while a depth measurement resolution of 5 mm fwhm effectively eliminates radial elongation. While these results were obtained with a depth independent measurement resolution, they suggest that the measurement resolution achieved by the present detector module will substantially reduce the radial elongation artifact for this PET camera geometry.

Large values of α are not necessarily desirable, even though equation 9 predicts that they improve position resolution at the photodiode end of the detector without harming the position resolution at the photomultiplier tube end, as large values of α impair the ability to correctly identify the crystal of interaction. When the interaction occurs at the photomultiplier tube end of the detector, the 511 keV signal observed by the photodiode is S/α and the photodiode signal to noise ratio is $S/N\alpha$. The dependence on the fraction of misidentified events on the signal to noise ratio in the photodiode in a 64 element detector has been reported previously [8]. Briefly summarized, when the signal to noise ratio is greater than 2:1, the fraction of events that are misidentified due to photodiode noise is negligible, but the misidentification fraction rises rapidly as the signal to noise falls below 2:1. This implies that $\alpha \leq S/2N$ in order to ensure proper identification independent of interaction position.

This LSO detector module has a light loss ratio $\alpha=5$, which is significantly larger than optimal and explains the large fraction of misidentified events. However, there is potential for improving the detector performance significantly, mainly by improving the reflector on the LSO crystal. The reflector material used was developed for BGO, and this work shows that a good reflector for BGO is not necessarily a good reflector for LSO! The maximum photodiode signal observed in the LSO module ($1200 e^-$) is significantly less than the $2000 e^-$ predicted based on the relative light outputs of BGO and LSO the relative photodiode quantum efficiencies at the different emission wavelengths. In addition, the photodiode noise can be reduced to $2/3$ of its present value with a better photodiode / amplifier combination. If these improvement goals are met (*i.e.* signal $S=2000 e^-$ and noise $N=350 e^-$), a detector with outstanding performance would result, as $\alpha=5$ would meet the $\alpha \leq S/2N$ criterion (giving a very low misidentification fraction) and give excellent depth of interaction measurement resolution (0.9 and 4.6 mm fwhm when excited at the photodiode and photomultiplier tube end of the crystal respectively, based on equation 9).

5. CONCLUSIONS

A PET detector module that uses an array of silicon photodiodes to both identify the crystal of interaction and measure the depth of interaction has been characterized. The module

uses LSO scintillator crystals in order to obtain sufficiently high signal to noise ratio to allow room temperature operation. A four element test module was constructed, and the average signal observed by the photomultiplier tube depended on the depth of interaction, varying smoothly over a 5:1 range. The signal observed in the photodiode averaged 1200 e⁻ per 511 keV photon interaction when excited at the photodiode end of the module, but was not discernible from the noise (a position independent 520 e⁻ fwhm) when excited at the photomultiplier tube end.

The ratio of the signals observed by the photodiode and the photomultiplier tube was used to measure the depth of interaction on an event by event basis. The accuracy of this depth measurement ranged from 4 mm fwhm at the photodiode end of the module (*i.e.* the patient end) to 13 mm at the photomultiplier tube end, in reasonable agreement with theoretical predictions. The module correctly identified the crystal of interaction 95% of the time when excited at the photodiode end, but only 73% of the time when excited at the photomultiplier tube end. All four detector elements have similar optical and electrical properties (little difference between elements is seen in Figures 3 and 4), suggesting that channel to channel variations will not be a major concern when constructing a detector module with a large number of elements.

The prospects for a very high performance detector module (0.9 to 4.6 mm depth of interaction measurement resolution and negligible misidentification) based on this concept is excellent. For this to occur, the maximum signal observed in the photodiode must be increased from 1200 e⁻ to 2000 e⁻ and the noise in the amplifier / photodiode combination reduced to 350 e⁻ fwhm. The improvement in the photodiode signal can be achieved by optimizing the reflector on the LSO crystal — the present coating was optimized for BGO and has a significantly lower light output than expected based on the relative light outputs of the two scintillator materials. Similarly, the improvement in noise is possible using standard, existing technology.

ACKNOWLEDGMENTS

We thank Mr. M. Ho of Lawrence Berkeley Lab for invaluable technical support, and Dr. R. Huesman of Lawrence Berkeley Lab for useful discussions. This work was supported in part by the Director, Office of Energy Research, Office of Health and Environmental Research, Medical Applications and Biophysical Research Division of the U.S. Department of Energy under contract No. DE-AC03-76SF00098, in part by the National Institutes of Health, National Heart, Lung, and Blood Institute, National Cancer Institute, and National Institute of Neurological Disorders and Stroke under grants No. P01-HL25840, No. R01-CA48002, and No. R01-NS29655.

REFERENCES

- [1] Hutchins GD. Mammographic PET (MAMPET): a dedicated imaging device for breast cancer applications. *Grant proposal to The Whitaker Foundation* pp. 28, 1993.
- [2] Thompson CJ, Murthy K, Weinberg IN, et al. Feasibility study for positron emission mammography. *Med. Phys.* **21**: pp. 529-538, 1994.
- [3] Moses WW and Derenzo SE. Design studies for a PET detector module using a PIN photodiode to measure depth of interaction. *IEEE Trans. Nucl. Sci.* **NS-41**: pp. 1441-1445, 1994.
- [4] Melcher CL, Schweitzer JS, Liberman A, et al. Temperature dependence of fluorescence decay time and emission spectrum of bismuth germanate. *IEEE Trans. Nucl. Sci.* **NS-32**: pp. 529-532, 1985.
- [5] Melcher CL and Schweitzer JS. Cerium-doped lutetium orthosilicate: A fast, efficient new scintillator. *IEEE Trans. Nucl. Sci.* **NS-39**: pp. 502-504, 1992.
- [6] Moses WW, Kipnis I and Ho MH. A 16-channel charge sensitive amplifier IC for a PIN photodiode array based PET detector module. *IEEE Trans. Nucl. Sci.* **NS-41**: pp. (submitted for publication), 1994.
- [7] Moses WW, Huesman RH and Derenzo SE. A new algorithm for using depth-of-interaction measurement information in PET data acquisition. *J. Nucl. Med.* **32**: pp. 995, 1991.
- [8] Moses WW, Derenzo SE, Nutt R, et al. Performance of a PET detector module utilizing an array of silicon photodiodes to identify the crystal of interaction. *IEEE Trans. Nucl. Sci.* **NS-40**: pp. 1036-1040, 1993.

